ACS APPLIED MATERIALS & INTERFACES

Research Article

www.acsami.org

Enhanced Photoelectrochemical Water Splitting Performance of Anodic TiO_2 Nanotube Arrays by Surface Passivation

Qunfang Gui,[†,‡,⊥] Zhen Xu,[†,§,⊥] Haifeng Zhang,[∥] Chuanwei Cheng,[∥] Xufei Zhu,[‡] Min Yin,[†] Ye Song,[‡] Linfeng Lu,[†] Xiaoyuan Chen,[†] and Dongdong Li*[,†]

[†]Shanghai Advanced Research Institute, Chinese Academy of Sciences, 99 Haike Road, Zhangjiang Hi-Tech Park, Pudong, Shanghai 201210, China

[‡]Key Laboratory of Soft Chemistry and Functional Materials of Education Ministry, Nanjing University of Science and Technology, Nanjing 210094, China

[§]University of Chinese Academy of Sciences, Beijing 100039, China

[∥]Shanghai Key Laboratory of Special Artificial Microstructure Materials, and Technology, School of Physics Science and Engineering, Tongji University, Shanghai 200092, China

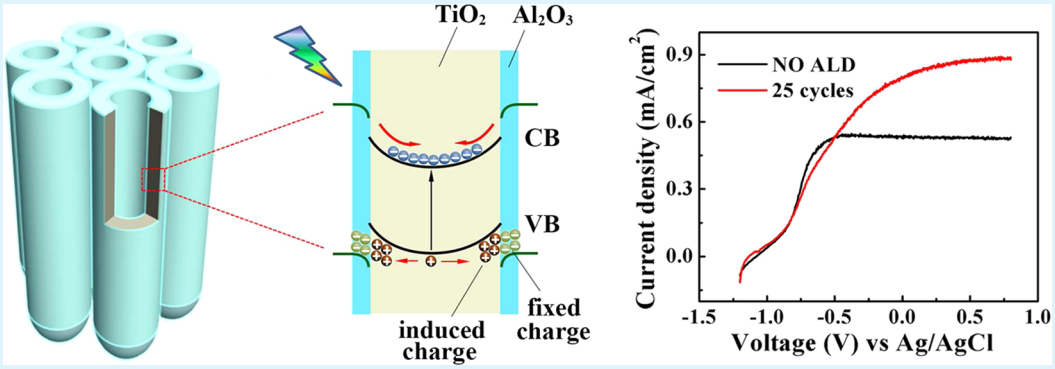

ABSTRACT: One-dimensional anodic titanium oxide nanotube (TONT) arrays provide a direct pathway for charge transport, and thus hold great potential as working electrodes for electrochemical energy conversion and storage devices. However, the prominent surface recombination due to the large amount surface defects hinders the performance improvement. In this work, the surface states of TONTs were passivated by conformal coating of high-quality Al_2O_3 onto the tubular structures using atomic layer deposition (ALD). The modified TONT films were subsequently employed as anodes for photoelectrochemical (PEC) water splitting. The photocurrent (0.5 V vs Ag/AgCl) recorded under air mass 1.5 global illumination presented 0.8 times enhancement on the electrode with passivation coating. The reduction of surface recombination rate is responsible for the substantially improved performance, which is proposed to have originated from a decreased interface defect density in combination with a field-effect passivation induced by a negative fixed charge in the Al_2O_3 shells. These results not only provide a physical insight into the passivation effect, but also can be utilized as a guideline to design other energy conversion devices.

KEYWORDS: *TiO_2 nanotubes, charge recombination, surface passivation, atomic layer deposition, photoelectrochemical water splitting*

INTRODUCTION

Self-organized anodic titanium oxide nanotube (TONT) films have been considered one of the most promising candidates in photovoltaic devices,[1,2] electrochromic windows,[3] photocatalysts,[4,5] and energy storage devices[6,7] due to their unique electrochemical, optical and electrical properties. As for the application in photoelectrochemical (PEC) water splitting, the solar-to-hydrogen conversion efficiency is mainly determined by efficient light absorption and charge transport. The improved light absorption capability has been demonstrated by a series of strategies including narrowing the bandgap[8] and geometry engineering.[9,10] The tubular structure of TONT, providing a direct pathway for electrons and ions transport, is beneficial for the efficient charge transport. However, the dilemma is that the PEC efficiency of TiO_2 electrodes is largely limited by the poor conductivity and charge carrier recombination. Recently, hydrogenated TiO_2 with induced oxygen vacancies has been extensively investigated, because it delivers substantially enhanced electrical conductivity[6] and photoresponse mainly in the UV region.[9,11,12] Because of the unique anodizing process, the substantial oxygen vacancies (i.e., Ti^{3+} donor states) known as the energetic disorder[13] (e.g., localized states in the band gap) are the main source of charge recombination in TONT.[14] The Ti^{3+} interstitials at the surface

Received: July 16, 2014
Accepted: September 8, 2014
Published: September 8, 2014

octahedrally coordinated to O, forming the Ti−O dangling bonds,[15] account for the surface trap sites. Then, the prominent electron−hole recombination loss caused by surface defect sites turns out to be one of the major obstacles in improving the PEC efficiency of TONT. Depressed electron−hole recombination has been realized by employing sacrificial electron donors, such as methanoic acid[16] and ethylene glycol,[17] in the electrolytes. However, a feasible method to passivate surface states without continuous supplying sacrificial agents is still highly desired.

High-κ dielectrics, such as Al_2O_3, SiO_2, and HfO_2, have shown excellent surface passivation properties on crystalline Si solar cells[18,19] and other electronic devices.[20] Recently, the surface passivation processes were introduced to electrochemical energy conversion devices,[21−23] with the aim of reducing surface charge recombination. In the case of PEC water splitting, surface passivation with assistance of atomic layer deposition (ALD) has been employed on Al_2O_3/Fe_2O_3,[22] Al_2O_3/WO_3[24] and TiO_2/TiO_2[21] electrodes showing promising results. However, few studies have systematically addressed the effect of deposition temperature and thickness of ALD Al_2O_3 on the PEC performance and the exact role of surface passivation. In this work, we investigate the PEC performances of TONT electrodes with ALD coated Al_2O_3 overlayers deposited at different temperatures and processing cycles. ALD coating delivered an enhanced photocurrent density by 1.8 times (0.5 V vs Ag/AgCl, 3 M KCl) with respect to the pristine TONT electrodes. The improved performances of TONT electrode is ascribed to the reduction of the electron−hole recombination because of the decreased interface defect density in combination with a field-effect passivation induced by a negative fixed charge in the Al_2O_3 shells.

EXPERIMENTAL SECTION

Fabrication of TONTs. Ti foils (99.7%, 0.2 mm thickness) were ultrasonically cleaned in acetone, ethanol, and deionized (DI) water successively for 10 min, respectively. All the TONT films were prepared by two-step anodization in an ethylene glycol electrolyte containing 0.3 wt % NH_4F and 2 vol % H_2O under 20 °C, as described in our previous literature.[1,6] In brief, the first-step anodization was performed at 60 V for 1 h in a conventional two-electrode configuration with a carbon rod as cathode electrode. The as-obtained TONT films were removed from the Ti foil by ultrasonication in deionized water for 10 min. The second-step anodization was carried out for 1 h under the same conditions. The as-prepared TONT samples were crystallized in ambient air at 150 °C for 2 h, then up to 450 °C for 3 h.

ALD Al_2O_3 Shell Deposition. The TONT samples were cleaned with DI water followed by drying in N_2 gas before ALD deposition. Al_2O_3 coatings on TONTs were performed with SUNALER-200 at different temperatures (100, 200, 300, and 400 °C) using trimethylaluminum ($Al(CH_3)_3$) and DI water as the precursors. The number of ALD cycles was varied from 10 to 200 with a growth rate of ∼1.04 Å/cycle.

Characterization. The morphology of nanotube films were characterized by field-emission scanning electron microscope (FESEM, FEI Quanta 600) and high resolution transmission electron microscope (HRTEM, JEM-2100F). PEC water splitting performances of the TONTs and TONTs with Al_2O_3 shells (denoted as TONT-A-cycle number) electrodes with active area of 1 cm^2 were evaluated by AUTOLAB PGSTAT302N/FRA2 in a three-electrode system at 25 °C using a Ag/AgCl (3 M KCl) reference electrode and a platinum wire counter electrode. Photocurrents were measured using a 300 W xenon lamp coupled with an AM 1.5 filter (PLS-SXE300/300UV) with 1 M potassium hydroxide (KOH) aqueous solution as supporting electrolyte. The incident photon-to-current conversion efficiencies (IPCE, DC mode) were measured in the above-mentioned three-electrode configuration by an AUTOLAB electrochemical station with the assistance of a commercial spectral response system (QEX10, PV Measurements). To acquire the stable photoresponse from photoanodes, we held each wavelength for 3 min before recording the photocurrent. Room temperature photoluminescence (PL) spectra of TONT electrodes were measured using a UV−vis spectrophotometer (iHR550), where a pulsed laser at 365 nm with an average power of 1 mW (150 fs, 80 MHz) was used as the excitation source.

RESULTS AND DISCUSSION

ALD method has been long considered as a chemical thin film deposition technique with precisely controlled conformal coating inside high aspect ratio nanochannels[25] and complex 3D nanoscaled structures.[26] Figure 1a−d shows the top and cross-sectional SEM images of TONT and TONT-A films. For easy characterization, the SEM observation is conducted on the TONT-A with 180 cycles of ALD coating (TONT-A-180). It can be seen that the inner diameter of TONTs becomes narrower (from 96.9 to 59.9 nm) after Al_2O_3 deposition. Note that the inner diameter of the tube decreases gradually from top to bottom due to the chemical etching effect,[1] as can be seen in Figure 1a,c. The inner diameter is further decreased from ∼78 to ∼30 nm after ALD deposition (Figure 1d). These results indicate that the inner surfaces are conformally coated by Al_2O_3 along the high aspect ratio nanotubes, which confirms that ALD is a powerful research tool for creating highly conformal layers on nanostructured electrodes. Figure 1e,f shows the HRTEM

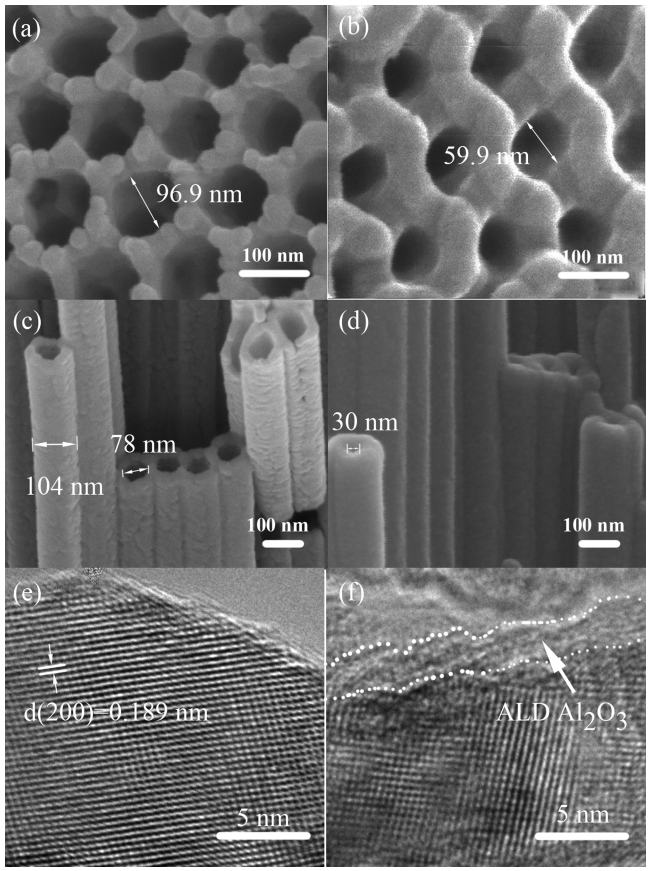

Figure 1. (a and b) Top and (c and d) cross-sectional SEM images of (a and c) TONT and (b and d) TONT-A-180. TEM images of (e) TONT and (f) TONT-A-25. Note: the ALD processing temperature is 200 °C.

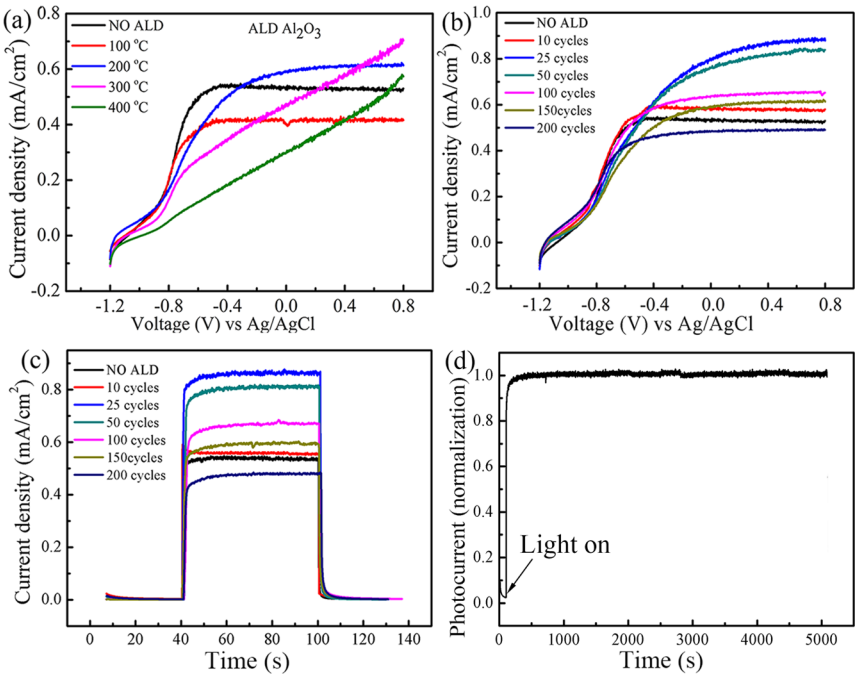

Figure 2. (a) Linear sweeps voltammetry (LSV) curves of (black) pristine TONT electrodes and TONT-A electrodes processed under (red) 100 °C, (blue) 200 °C, (magenta) 300 °C, and (green) 400 °C. (b) LSV curves and (c) photocurrent responses of TONT and TONT-A electrodes with different ALD coating cycles in 1 M KOH solution under the illumination of a 300 W Xe lamp coupled with an AM1.5 filter. (d) Longtime stability of TONT-A-25 electrode by recording the photocurrent for 5000 s in 1 M KOH aqueous solution under an applied potential of 0.5 V vs Ag/AgCl and an illumination of a 300 W Xe lamp.

images of TONT and TONT-A-25 films, from which the well-resolved (200) lattice fringes (d = 0.189 nm) can be seen in both samples, indicating the well-crystallized structure. The overlayer (labeled by a white arrow in Figure 1f) indicates the amorphous characteristics of Al_2O_3 shell with an average thickness of about 2.6 nm.

The electrical properties of composite electrodes are strongly dependent on the ALD deposition temperature and film thickness.[21,27] The PEC performance of TONT-A as a function of processing temperatures of 100, 200, 300, and 400 °C is first investigated on the electrodes with 150 cycles coating. It was found that the photocurrent is strongly correlated with the deposition temperature. After ALD at 100 °C, the photocurrent of the electrode decreases compared with that of the pristine TONT (Figure 2a), while the photocurrent increases up to 0.6 mA/cm^2 (0.5 V vs Ag/AgCl) at 200 °C. As the temperature further increases to 300 and 400 °C, the PEC performances of TONT-A electrodes tend to decrease even worse than that of the pristine TONT electrode. As for the TONT-A electrode deposited at 100 °C, the inferior PEC performance may be ascribed to the positive charges located at the interface,[27] which somehow expels the holes to the bulk and facilitates its recombination with electrons, whereas there are negative charges located at the interface when deposited at 200 °C or higher,[27] which facilitates accumulated holes at the nanotube surface and creates a highway for electrons to migrate to the cathode. On the other hand, the deposition temperature also affects the composition of the ALD shell, which mainly consists of $AlHO_x$.[28,29] It has been reported that hydrogen from the Al_2O_3 bulk could diffuse and provide chemical passivation at the interface, thereby reducing defect-related recombination.[28] Studies have also shown that as deposition temperature increases higher than 200 °C, the concentration of hydrogen atoms decreases, and consequently, chemical passivation become weaker.[29] This could interpret the optimized deposition temperature of 200 °C.

The PEC performance of TONT-A electrodes are subsequently investigated by varying the ALD cycles at 10, 25, 50, 100, 150, and 200 cycles under 200 °C. Figure 2b,c represents the LSV curves and photocurrent responses at a constant potential of 0.5 V (vs Ag/AgCl) as a function of Al_2O_3 shell thickness, respectively. TONT-A-10 electrode shows a slight increase in photocurrent compared to that of the pristine TONT electrode (Figure 2b). The photocurrent achieves a maximum value of 0.9 mA/cm^2 (0.5 V vs Ag/AgCl) for the TONT-A-25 electrode, which is 0.8 times higher than that of the pristine TONT electrode. However, as the shell thickness continues to increase, the photocurrent begins to decrease gradually and is even less than that of pristine TONT when coating for 200 ALD cycles. The trend of photocurrent responses in Figure 2c mirrors that of the LSV plots. The inferior performance of the TONT-A-10 sample, compared with the TONT-A-25 electrode, may be ascribed to the incomplete coverage of the dangling bonds on the surface of TONT. After 25 cycles of deposition, most of surface trap sites are believed to be covered, resulting in the highest photocurrent. When the number of cycles is greater than 25 (50−200 cycles), the photocurrent decrease, revealing that the thickness of alumina has exceeded the tunneling thickness (~2 nm)[30] and thereby leads to a decrease in PEC performance than that of the TONT-A-25. The following measurements will be performed on TONT-A-25 and pristine TONT electrodes.

The thermodynamic instability of Al_2O_3 in base electrolyte will determine the practical applications. Sivula and co-workers have reported the Fe_2O_3 electrode covered by an ALD Al_2O_3 layer, which displayed stable behavior in 1 M KOH for more than 30 min under an applied potential of 1.03 V vs RHE and 1 sun illumination.[22] Herein, long-time stability of the TONT-A

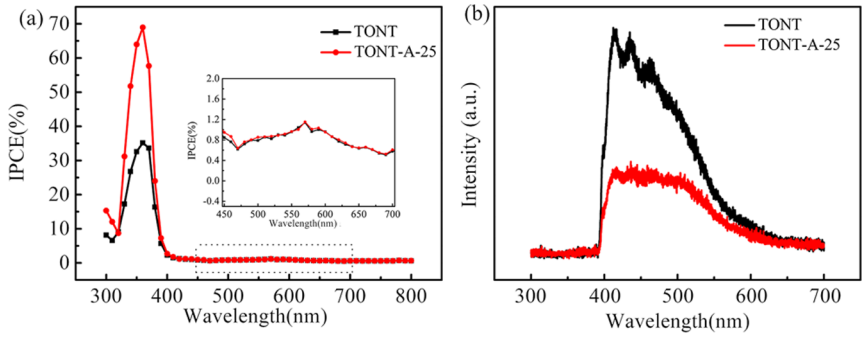

Figure 3. (a) IPCE spectra of TONT and TONT-A-25 electrode in the range of 300−800 nm at 0 V (vs Ag/AgCl); (inset) magnified IPCE spectra at wavelengths of 430−700 nm, as highlighted in dashed box. (b) Photoluminescence (PL) spectra of TONT and TONT-A-25.

electrode is also tested by recording the photocurrent for 5000 s in 1 M KOH aqueous solution (pH = 13.6) under an applied potential of 0.5 V (vs Ag/AgCl) and an illumination of a 300 W Xe lamp. It can be observed in Figure 2d that the TONT-ALD electrode is stable for the entire duration of characterization. The result further demonstrates that the ALD of Al_2O_3 is sufficiently stable in long-time application under harsh water splitting conditions.

IPCE measurements were carried out to investigate the contribution of each monochromatic light to the photocurrent density. Compared with the measurements based on the wide band light source with the absence of reliable calibration, the intensity-independent IPCE provides a reliable method to characterize the wavelength dependent photoresponse. The IPCE is calculated as a function of wavelength using IPCE = $((1240\ \text{mW·nm/mA})I)/(\lambda J_{light})$, where λ is the incident light wavelength (nm), and I and J_{light} are the photocurrent density (mA/cm^2) and incident light irradiance (mW/cm^2) at a specific wavelength, respectively.[11] Figure 3a shows the IPCE plots of TONT and TONT-A-25 at a zero bias vs Ag/AgCl reference electrode. The results indicate that the enhanced photocurrent is mainly contributed by UV light response. The ALD coating of Al_2O_3 shell gives rise to a pronounced enhancement of IPCE in the whole UV region (300−400 nm) with a maximum of 70% at 360 nm. A broad band weak photoactivity of pristine TONT nanotube in 400−600 nm could be ascribed to fluorine doping during anodization in NH_4F containing electrolytes.[21,31] In addition, the coating independent visible light response indicates the surface passivation contributes little on the interband transition.

To further investigate the role of ALD coating on the PEC performance, we carried out the photoluminescence (PL) experiments with a 365 nm pulsed laser as excitation source. PL spectra are often used to study the surface processes involving electron−hole recombination of semiconductors.[32] The broad-band emission around 410 nm, as shown in Figure 3b, can be assigned to the recombination of photoexcited holes with electrons occupying the singly ionized oxygen vacancies in TiO_2.[33] Apparently, the PL intensity of the TONT-A-25 sample decreases remarkably compared with pristine TONT, which can be ascribed to the reduction of the recombination process after the Al_2O_3 coating.[34]

Because of the unique fabrication method of TONT, titanium interstitials on the surface due to titanium excess and F anions doping[14] are usually surrounded by distorted O octahedral forming the Ti−O dangling bonds,[15] which act as charge carrier traps and recombination centers, while the ALD layer of Al_2O_3 can effectively decrease the defect states by saturating the dangling bonds and thus increases the PEC performance of the corresponding electrodes.[28,35]

In addition to the chemical passivation effect, a strong field-effect passivation by shielding the minority carriers from the semiconductor interface plays an important role in the *p*-type crystalline Si passivation mechanism.[19] The built-in electric field attributed to the presence of a high negative fixed charge density is originated from the intrinsic (Al vacancies and O interstitials) and extrinsic (interstitial H) defects in Al_2O_3.[18,36] Indeed, the presence of negative fixed charge in Al_2O_3 can also benefit for the surface passivation of *n*-type TONT electrode for PEC application. Figure 4 shows a schematic of the field-effect passivation in the presence of Al_2O_3 layer. Under UV light illumination, the photogenerated holes present in the TiO_2 valence band will be transferred to the interface between TiO_2 and ALD layer because of the presence of the negative charges that localized in the Al_2O_3 film close to the interface with TiO_2. The as-formed electron depletion at the nanotube surface induces surface band bending and further suppress the electrons from capturing by the surface trap states, as shown in right panel of Figure 4. Such coupled mechanisms (chemical passivation and field effect passivation) will spatially separate the photogenerated electron−holes with suppressed photo-carrier recombination and dramatically prolonged carrier lifetimes. The unpaired electrons would migrate to the cathode

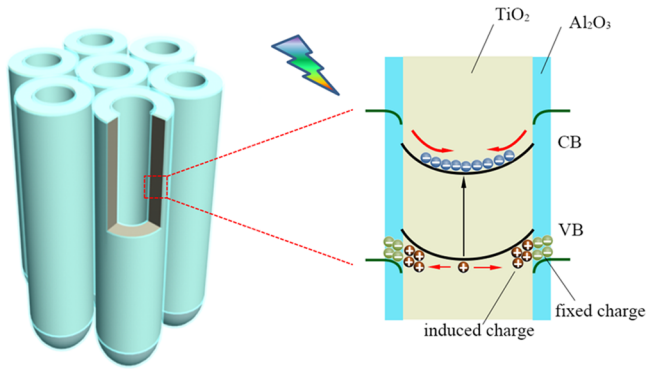

Figure 4. Schematic diagram of the field-effect passivation by Al_2O_3 coating. (Left) Illustration of the structure of the (tan) TONT deposited with (powder blue) Al_2O_3 shell. (Right) Energy band diagram of TONT coated with Al_2O_3 shell, where VB and CB are the valence and conduction bands, respectively. Under UV irradiation, photogenerated holes are trapped at the surface due to the presence of the negative charges located in the Al_2O_3 film, leaving behind unpaired electrons in the center of tube wall.

through the nanotube array's backbone to participate in the water reduction reaction with much suppressed recombination.

CONCLUSIONS

In conclusion, the PEC performances of TONT electrodes with ALD-coated Al_2O_3 overlayers have systematically been functions of processing temperature and deposition cycle. The optimized ALD coating delivered an enhanced photocurrent density by 0.8 times with respect to the pristine TONT electrodes, mainly contributed by the remarkably increased photoresponse in the UV region. The improved performances of TONT-A electrode is ascribed to the reduction of the electron−hole recombination because of the decreased surface defect density in combination with field-effect passivation induced by a negative fixed charge in the Al_2O_3 shells. The mechanism insight gained from this study, with tunable electronic properties of nanoscaled materials, would provide a guideline for both high-performance photoelectrochemical and optoelectronic devices.

AUTHOR INFORMATION

Corresponding Author

*E-mail: lidd@sari.ac.cn.

Author Contributions

⊥G.U. and Z.X. contributed equally.

Notes

The authors declare no competing financial interest.

ACKNOWLEDGMENTS

This work is financially supported by the National Natural Science Foundation of China (Grants 61171043, 51077072, 11174308, and 51102271) and by Shell Global Solutions International B.V. (PT31045).

REFERENCES

(1) Li, D. D.; Chang, P. C.; Chien, C. J.; Lu, J. G. Applications of Tunable TiO_2 Nanotubes as Nanotemplate and Photovoltaic Device. *Chem. Mater.* **2010**, *22*, 5707−5711.

(2) Tao, L.; Xiong, Y.; Liu, H.; Shen, W. Z. High Performance PbS Quantum Dot Sensitized Solar Cells via Electric Field Assisted in Situ Chemical Deposition on Modulated TiO_2 Nanotube Arrays. *Nanoscale* **2014**, *6*, 931−938.

(3) Yao, D. D.; Field, M. R.; O'Mullane, A. P.; Kalantar, K.; Ou, J. Z. Electrochromic Properties of TiO_2 Nanotubes Coated with Electrodeposited MoO_3. *Nanoscale* **2013**, *5*, 10353−10359.

(4) Yu, D. L.; Zhu, X. F.; Xu, Z.; Zhong, X. M.; Gui, Q. F.; Song, Y.; Zhang, S. Y.; Chen, X. Y.; Li, D. D. Facile Method to Enhance the Adhesion of TiO_2 Nanotube Arrays to Ti Substrate. *ACS Appl. Mater. Interfaces* **2014**, *6*, 8001−8005.

(5) Liu, N.; Schneider, C.; Freitag, D.; Hartmann, M.; Venkatesan, U.; Muller, J.; Spiecker, E.; Schmuki, P. Black TiO_2 Nanotubes: Cocatalyst-Free Open-Circuit Hydrogen Generation. *Nano Lett.* **2014**, *14*, 3309−3313.

(6) Wu, H.; Xu, C.; Xu, J.; Lu, L. F.; Fan, Z. Y.; Chen, X. Y.; Song, Y.; Li, D. D. Enhanced Supercapacitance in Anodic TiO_2 Nanotube Films by Hydrogen Plasma Treatment. *Nanotechnology* **2013**, *24*, 455401−455407.

(7) Li, H.; Chen, Z. H.; Tsang, C. K.; Li, Z.; Ran, X.; Lee, C.; Nie, B.; Zheng, L. X.; Hung, T. F.; Lu, J.; Pan, B. C.; Li, Y. Y. Electrochemical Doping of Anatase TiO_2 in Organic Electrolytes for High-Performance Supercapacitors and Photocatalysts. *J. Mater. Chem. A* **2014**, *2*, 229−236.

(8) Dong, F.; Guo, S.; Wang, H. Q.; Li, X. F.; Wu, Z. B. Enhancement of the Visible Light Photocatalytic Activity of C-Doped TiO_2 Nanomaterials Prepared by a Green Synthetic Approach. *J. Phys. Chem. C* **2011**, *115*, 13285−13292.

(9) Chen, B.; Hou, J.; Lu, K. Formation Mechanism of TiO_2 Nanotubes and Their Applications in Photoelectrochemical Water Splitting and Supercapacitors. *Langmuir* **2013**, *29*, 5911−5919.

(10) Lin, J.; Liu, K.; Chen, X. Y. Synthesis of Periodically Structured Titania Nanotube Films and Their Potential for Photonic Applications. *Small* **2011**, *7*, 1784−1789.

(11) Xu, C.; Song, Y.; Lu, L. F.; Cheng, C. W.; Liu, D. F.; Fang, X. H.; Chen, X. Y.; Zhu, X. F.; Li, D. D. Electrochemically Hydrogenated TiO_2 Nanotubes with Improved Photoelectrochemical Water Splitting Performance. *Nanoscale Res. Lett.* **2013**, *8*, 391−397.

(12) Wang, G. M.; Wang, H. Y.; Ling, Y. C.; Tang, Y. C.; Yang, X. Y.; Fitzmorris, R. C.; Wang, C. C.; Zhang, J. Z.; Li, Y. Hydrogen-Treated TiO_2 Nanowire Arrays for Photoelectrochemical Water Splitting. *Nano Lett.* **2011**, *11*, 3026−3033.

(13) Villanueva, J.; Jang, S. R.; Halverson, A. F.; Zhu, K.; Frank, A. J. Trap-Free Transport in Ordered and Disordered TiO_2 Nanostructures. *Nano Lett.* **2014**, *14*, 2305−2309.

(14) Richter, C.; Schmuttenmaer, C. A. Exciton-Like Trap States Limit Electron Mobility in TiO_2 Nanotubes. *Nat. Nanotechnol.* **2010**, *5*, 769−772.

(15) Shibata, N.; Goto, A.; Choi, S.-Y.; Mizoguchi, T.; Findlay, S.; Yamamoto, T.; Ikuhara, Y. Direct Imaging of Reconstructed Atoms on TiO_2 (110) Surfaces. *Science* **2008**, *322*, 570−573.

(16) Tada, H.; Teranishi, K.; Ito, S. Additive Effect of Sacrificial Electron Donors on Ag/TiO_2 Photocatalytic Reduction of Bis(2-dipyridyl)disulfide to 2-Mercaptopyridine in Aqueous Media. *Langmuir* **1999**, *15*, 7084−7087.

(17) Liu, Z. Y.; Pesic, B.; Raja, K. S.; Rangaraju, R. R.; Misra, M. Hydrogen Generation under Sunlight by Self Ordered TiO_2 Nanotube Arrays. *Int. J. Hydrogen Energy* **2009**, *34*, 3250−3257.

(18) Hoex, B.; Gielis, J. J. H.; De Sanden, M. C. M. V.; Kessels, W. M. M. On the *c*-Si Surface Passivation Mechanism by the Negative-Charge-Dielectric Al_2O_3. *J. Appl. Phys.* **2008**, *104*, 113703−113709.

(19) Terlinden, N. M.; Dingemans, G.; de Sanden, M. C. M. V.; Kesselsa, W. M. M. Role of Field-Effect on *c*-Si Surface Passivation by Ultrathin (2−20 nm) Atomic Layer Deposited Al_2O_3. *Appl. Phys. Lett.* **2010**, *96*, 112101−112103.

(20) Chang, P. C.; Fan, Z. Y.; Chien, C. J.; Stichtenoth, D.; Ronning, C.; Lu, J. G. High-Performance ZnO Nanowire Field EffecTransistors. *Appl. Phys. Lett.* **2006**, *89*, 133113−133115.

(21) Hwang, Y. J.; Hahn, C.; Liu, B.; Yang, P. D. Photoelectrochemical Properties of TiO_2 Nanowire Arrays: A Study of the Dependence on Length and Atomic Layer Deposition Coating. *ACS Nano* **2012**, *6*, 5060−5069.

(22) Le Formal, F.; Tetreault, N.; Cornuz, M.; Moehl, T.; Gratzel, M.; Sivula, K. Passivating Surface States on Water Splitting Hematite Photoanodes with Alumina Overlayers. *Chem. Sci.* **2011**, *2*, 737−743.

(23) Lin, C.; Tsai, F. Y.; Lee, M. H.; Lee, C. H.; Tien, T. C.; Wang, L. P.; Tsai, S. Y. Enhanced Performance of Dye-Sensitized Solar Cells by an Al_2O_3 Charge-Recombination Barrier Formed by Low-Temperature Atomic Layer Deposition. *J. Mater. Chem.* **2009**, *19*, 2999−3003.

(24) Kim, W.; Tachikawa, T.; Monllor, D.; Kim, H. I.; Majima, T.; Choi, W. Promoting Water Photooxidation on Transparent WO_3 Thin Films Using an Alumina Overlayer. *Energy Environ. Sci.* **2013**, *6*, 3732−3739.

(25) Elam, J. W.; Xiong, G.; Han, C. Y.; Wang, H. H.; Birrell, J. P.; Welp, U.; Hryn, J. N.; Pellin, M. J.; Baumann, T. F.; Poco, J. F.; Satcher, J. H. Atomic Layer Deposition for the Conformal Coating of Nanoporous Materials. *J. Nanomater.* **2006**, 64501−64505.

(26) Xia, X. H.; Zeng, Z. Y.; Li, X. L.; Zhang, Y. Q.; Tu, J. P.; Fan, N. C.; Zhang, H.; Fan, H. J. Fabrication of Metal Oxide Nanobranches on Atomic-Layer-Deposited TiO_2 Nanotube Arrays and Their Application in Energy Storage. *Nanoscale* **2013**, *5*, 6040−6047.

(27) Rafi, J. M.; Zabala, M.; Beldarrain, O.; Campabadal, F. Deposition Temperature and Thermal Annealing Effects on the Electrical Characteristics of Atomic Layer Deposited Al_2O_3 Films on Silicon. *J. Electrochem. Soc.* **2011**, *158*, G108−G114.

(28) Hoex, B.; Heil, S. B. S.; Langereis, E.; Van, M. C. M.; Kessels, W. M. M. Ultralow Surface Recombination of *c*-Si Substrates Passivated by Plasma-Assisted Atomic Layer Deposited Al_2O_3. *Appl. Phys. Lett.* **2006**, *89*, 042112−042114.
(29) Dingemans, G.; van de Sanden, M. C. M.; Kessels, W. M. M. Influence of the Deposition Temperature on the *c*-Si Surface Passivation by Al_2O_3 Films Synthesized by ALD and PECVD. *Electrochem. Solid-State Lett.* **2010**, *13*, H76−H79.
(30) Ganapathy, V.; Karunagaran, B.; Rhee, S. W. Improved Performance of Dye-Sensitized Solar Cells with TiO_2/Alumina Core-Shell Formation Using Atomic Layer Deposition. *J. Power Sources* **2010**, *195*, 5138−5143.
(31) Park, H.; Choi, W. Effects of TiO_2 Surface Fluorination on Photocatalytic Reactions and Photoelectrochemical Behaviors. *J. Phys. Chem. B* **2004**, *108*, 4086−4093.
(32) Wang, H.; Bai, Y. S.; Zhang, H.; Zhang, Z. H.; Li, J. H.; Guo, L. CdS Quantum Dots-Sensitized TiO_2 Nanorod Array on Transparent Conductive Glass Photoelectrodes. *J. Phys. Chem. C* **2010**, *114*, 16451−16455.
(33) Ye, M. D.; Gong, J. J.; Lai, Y. K.; Lin, C. J.; Lin, Z. Q. High-Efficiency Photoelectrocatalytic Hydrogen Generation Enabled by Palladium Quantum Dots-Sensitized TiO_2 Nanotube Arrays. *J. Am. Chem. Soc.* **2012**, *134*, 15720−15723.
(34) Li, X. Z.; Li, F. B. Study of Au/Au^{3+}-TiO_2 Photocatalysts toward Visible Photooxidation for Water and Wastewater Treatment. *Environ. Sci. Technol.* **2001**, *35*, 2381−2387.
(35) Suh, D.; Weber, K. Effective Silicon Surface Passivation by Atomic Layer Deposited Al_2O_3/TiO_2 Stacks. *Phys. Status Solidi RRL* **2014**, *8*, 40−43.
(36) Matsunaga, K.; Tanaka, T.; Yamamoto, T.; Ikuhara, Y. First-Principles Calculations of Intrinsic Defects in Al_2O_3. *Phys. Rev. B* **2003**, *68*, 085110−085118.